13èmes Journées de l'Hydrodynamique
21 - 23 novembre 2012
Laboratoire d'Hydraulique Saint-Venant
Ile des Impressionnistes,
Chatou (78), France

MODÉLISATION HYDRODYNAMIQUE DES SYSTÈMES HOULOMOTEURS OSCILLANTS

HYDRODYNAMIC MODELLING OF OSCILLATING WAVE ENERGY CONVERTERS

F. DIAS[*,], E. RENZI[**]**

[*] CMLA, Ecole Normale Supérieure de Cachan, 94235 Cachan, France
[**] UCD School of Mathematical Sciences,
University College Dublin, Belfield, Dublin 4, Ireland
frederic.dias@ucd.ie

Résumé

Cet article analyse la dynamique des machines houlomotrices de type grand volet situées près du littoral. Deux configurations différentes sont étudiées. La première est un houlomoteur unique placé au milieu d'un canal rectiligne, tandis que la seconde est un réseau périodique de houlomoteurs. La première configuration recrée la disposition habituelle des expériences à petite échelle dans les canaux à houle, tandis que la seconde fournit un schéma théorique pour le développement de fermes. Dans le cadre de la théorie linéaire non visqueuse en écoulement potentiel, l'application du théorème de Green donne une équation intégrale hyper singulière du potentiel de vitesse dans le domaine fluide. La solution est trouvée en termes d'une série convergeant rapidement de polynômes de Chebyshev. Il est montré que la résonnance des ondes transversales dans les deux dispositions est bénéfique pour accroître la performance du système.

Summary

This paper analyses the dynamics of large flap-type wave energy converters in the nearshore. Two configurations are investigated, both relevant to practical applications. In the first one, a single converter is placed in the middle of a channel, while in the second one a periodic array of converters is considered. The first configuration recreates the usual layout of small-scale experiments in wave tanks, while the second one provides a theoretical scheme for on-site development of wave farms. With a linear inviscid potential-flow theory, application of Green's theorem yields a hypersingular integral equation for the velocity potential. The solution is found in terms of a series of Chebyshev polynomials of the second kind. The resonance of transverse waves in both layouts is beneficial for increasing the performance of the systems.

I – Introduction

Bottom hinged flaps are efficient means for extracting power from ocean waves [1, 2]. One of the most promising devices belonging to this category is the Oscillating Wave Surge Converter. The latter is made by a buoyant flap hinged on a foundation at the bottom of the ocean, pitching under the action of incoming waves. The device is linked to a generator, which enables power capture from incident waves. The flap width w is much larger than the wave amplitude A and is comparable to the wavelength λ, so that the body is regarded as *large*. When hit by waves, a large body alters the pattern of the incoming waves and produces substantial diffraction. The OWSC achieves consistent efficiency levels due to the high diffraction loads acting on the large flap surface, which govern the system performance curve [3]. Hence the OWSC is a large, torque-driven device and differs from small devices which base their capacity on radiation properties, like for example heaving buoys. As a consequence, the dynamics of the OWSC cannot be fully characterised by employing existing theories valid for small floats – like the point-absorber theory [4] – but must be described in a different fashion.

Renzi & Dias [5, 6, and 7] derived a new semi-analytical model of the OWSC and investigated its behaviour in several configurations of practical interest. Here we shall first review the model of [5] and [6] for the OWSC in a channel and for a periodic array of OWSCs, respectively. Then we shall discuss the features of such layouts and the unique properties which make them differ from analogous systems of other devices.

Under normally incident waves, the channel and array configurations correspond to the same analytical problem [8], which is briefly summarised and solved in Section II. In Section III – 1, the channel configuration is considered and the effect of the channel lateral walls on the performance of the device is investigated. In Section III – 2, the array configuration is analysed as a model for a large wave farm. It is shown that there exists an optimum spacing between the flaps, which maximises the power capture of the farm. In such configuration there are no transverse propagating modes far from the array, so that energy leakage in the far field is minimised.

II – Mathematical model

The basis of the mathematical model for the OWSC is provided by [5] and briefly summarized here. The device is a rectangular box of width w, hinged along a straight foundation at distance c from the bottom of an ocean of constant depth h. The device is in the middle of a channel of total width b, as shown in figure 1. The flap thickness is mathematically immaterial for the calculation of the velocity potential [5]. Monochromatic waves of amplitude A_I and frequency ω are incoming from the right and have wave crests parallel to the flap. As already mentioned, because of the mirroring effect of the channel lateral walls, the model also represents an infinite array of OWSCs with spatial period b. A plane reference system of coordinates (x, y, z) is also set, with x on the centre line of the channel, y along the axis of the plate at rest position and z positive upwards. Assume the fluid is inviscid, the flow irrotational and the perturbation time harmonic with period T and frequency $\omega = 2\pi/T$. Hence there exists a velocity potential

$$\Phi(x, y, z, t) = \mathrm{Re}\{\phi(x, y, z)e^{-i\omega t}\}, \tag{1}$$

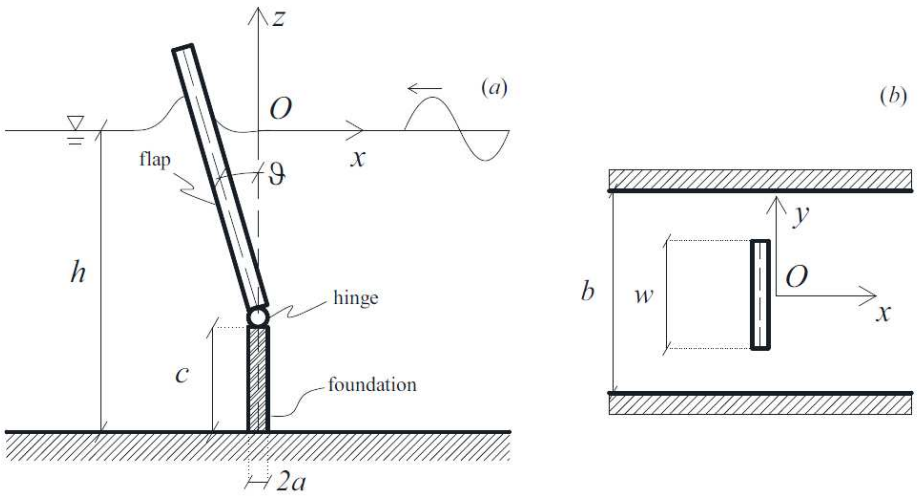

Figure 1- Geometry of the system (channel layout) : (a) section, (b) plan view.

where ϕ is the complex spatial potential. Within the framework of a linear potential-flow theory, the potential $\phi = \phi_S + \phi_R$ is the sum of the scattering potential ϕ_S, solution of the scattering problem where the flap is fixed in incoming waves, and the radiation potential ϕ_R. The latter solves the radiation problem, in which the flap is forced to oscillate without incident waves. In the following, the two problems are considered separately and their solutions added to get the total potential.

II – 1 The scattering problem

Following [5], the scattering potential is the solution of the boundary-value problem made by the Laplace equation, the kinematic-dynamic boundary condition on the free surface and the no flux conditions on the bottom and on the flap, respectively

$$\nabla^2\phi_S = 0 \tag{2a}$$

$$\phi_{S,z} - \frac{\omega^2}{g}\phi_S = 0, \qquad z = 0 \tag{2b}$$

$$\phi_{S,z} = 0, \qquad z = -h \tag{2c}$$

$$\phi_{S,x} = 0, \qquad x = \pm 0, |y| < w/2, \tag{2d}$$

where the subscripts with commas indicate differentiation with the relevant variables [see also 9, pag. 357]. Assuming $\phi_S = \phi_D + \phi_I$, where

$$\phi_I = -i\frac{gA_I}{\omega}\frac{\cosh k(z+h)}{\cosh kh}e^{-ikx} \tag{3}$$

is the spatial potential of the incident wave, k is the real solution of the dispersion relation $\omega^2 = gk\tanh kh$ and g the acceleration due to gravity, the unknown diffraction potential ϕ_D, outgoing at large $|x|$, can be determined by applying the Green integral theorem to the governing equations (2a) – (2d). Such procedure yields an integral equation with a singular kernel, which is de-singularised via a series expansion in terms of the Chebyshev polynomials of the second kind and even order U_{2p}, $p = 0,1, \ldots, P$ [see Appendix A of 5], thus yielding

$$\phi_D(x,y,z) = -\frac{1}{4\sqrt{2}}igA_I bwkx\frac{\cosh k(z+h)}{\left(gh + \frac{g}{\omega^2}\sinh^2 kh\right)^{\frac{1}{2}}}$$

$$\times \sum_{p=0}^{P} \beta_{2p} \sum_{m=-\infty}^{+\infty} \int_{-1}^{1} (1-u^2)^{\frac{1}{2}} U_{2p}(u) \frac{H_1^{(1)}\left(k\sqrt{x^2+\left(y-\frac{1}{2}wu-bm\right)^2}\right)}{\sqrt{x^2+\left(y-\frac{1}{2}wu-bm\right)^2}}\, du. \qquad (4)$$

In the latter expression, $H_1^{(1)}$is the Hankel function of the first kind and first order, outgoing for large argument, while the β_{2p} are the complex solutions of a linear system of equations which stems from the boundary condition on the flap (2d). The system is solved numerically with a collocation scheme [see 5], so that the solution (4) is partially numerical.

II – 2 The radiation problem

The radiation potential $\phi_R$must satisfy again the governing equation (2a), the boundary conditions on the free surface (2b) and on the bottom (2c) and the kinematic condition on the flap:

$$\phi_{R,x} = i\omega\Theta\,(z+h-c)H(z+h-c), \qquad x = \pm 0, |y| < \frac{w}{2}, \qquad (5)$$

where $\theta(t) = \mathrm{Re}\{\Theta e^{-i\omega t}\}$ is the rotation of the flap and H is the Heaviside step function, which in (5) assures absence of flux through the bottom foundation (see again figure 1). This system of equations is solved with the same procedure as above, thus yielding

$$\phi_R(x,y,z) = \frac{1}{4\sqrt{2}}\Theta w\omega b^2 \sum_{n=0}^{+\infty} \kappa_n\, x \frac{\cosh\kappa_n(z+h)}{\left(h/b+\frac{g}{b\omega^2}\sinh^2\kappa_n h\right)^{\frac{1}{2}}}$$
$$\times \sum_{p=0}^{P} \alpha_{(2p)n} \sum_{m=-\infty}^{+\infty} \int_{-1}^{1} (1-u^2)^{\frac{1}{2}} U_{2p}(u) \frac{H_1^{(1)}\left(\kappa_n\sqrt{x^2+\left(y-\frac{1}{2}wu-bm\right)^2}\right)}{\sqrt{x^2+\left(y-\frac{1}{2}wu-bm\right)^2}}\, du. \qquad (6)$$

In the latter expression, $\kappa_0 = k$, while $\kappa_n = ik_n$ is the solution of the dispersion relation $\omega^2 = -gk_n \tan k_n h$ for the vertical eigenmodes of the system [see 9]. Finally, the $\alpha_{(2p)n}$ are the complex solutions of a system of linear equations which stems from (5).

II – 3 The body motion

The motion of the flap is governed by Newton's law:

$$(I+\mu)\theta_{tt}(t) + \left(\nu+\nu_{pto}\right)\theta_t(t) + C\theta(t) = \mathcal{F}(t) \qquad (7)$$

[see 5 for details]. In (7), I is the moment of inertia of the flap, C the buoyancy torque and $\nu_{pto}$the damping coefficient of the generator (all assumed to be given by the manufacturer). Furthermore, in expression (7) μ denotes the added inertia torque, ν the radiation damping and $\mathcal{F}$ the exciting torque acting on the plate, which are determined from (5) and (6) as shown in Section 2 of [5] (see eq.s 2.34, 2.35 and 2.36, respectively). The average generated power over a period $T = 2\pi/\omega$ is given by

$$P = \frac{1}{T}\int_0^T \nu_{pto}\theta_t^2\, dt, \tag{8}$$

from which the capture factor

$$C_F = \frac{P}{\frac{1}{2}\rho g A_I^2 C_g w} \tag{9}$$

is defined as the ratio between the generated power per unit flap width and the incident power per unit crest length, C_g being the group velocity of the incident waves.

III – Discussion

In this section discussion is undertaken for two different systems. In the first one, a single flap is placed in the middle of a straight channel, as depicted in figure 1. In the second one, an infinite array of flaps is placed in the open ocean, as represented in figure 2. Under normally incident waves, both systems have the same analytical solution derived in Section II [see 5, 6]. In practical applications, however, the channel and the array configurations are different. The first one represents the usual layout of experiments in wave tank aiming at reproducing the behaviour of the flap in the ocean [see 1]. Here the position of the lateral walls is fixed and the width of the device can be varied. The second layout represents a large farm of converters in the open ocean. Here the practical issue is to determine the optimum spacing between the devices in order to maximise the capture factor of the system.

III – 1 A single flap in a channel

For a single flap in a channel, the capture factor curve shows a characteristic spiky behaviour, as depicted in figure 3. Here the values of C_F are reported versus the period of the incident waves, being $h = 10.9\, m$, $c = 1.5\, m$ and $A_I = 0.3\, m$, for several flap widths. Note that the capture factor curves all have spikes at the cut-off periods of the channel sloshing modes:

$$T_m = \sqrt{\frac{2\pi b}{mg\tanh\left(\frac{2m\pi h}{b}\right)}} \tag{10}$$

with $m = 1,2,\ldots$ As already shown by [5], when the period of the incident waves approaches the cut-off period of the m-th sloshing mode (10), the latter turns from propagating along the channel to evanescent, i.e. trapped near the flap. This results in an increase of the hydrodynamic action on the flap, ultimately determining the spikes of the capture factor curve shown in figure 3. In the latter, the effect of increasing the flap width is also noticeable. As long as the flap width is small compared to the channel width, increasing w has the

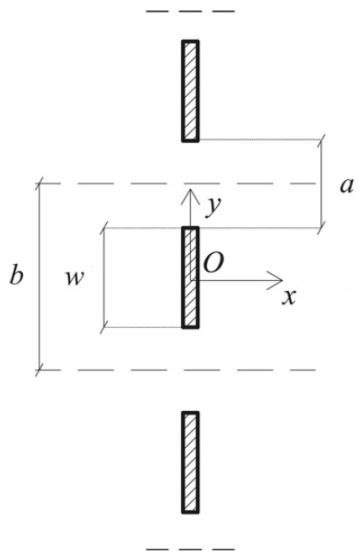

Figure 2 - Plan view of the array configuration. The dashed lines at both sides of the reference flap represent imaginary waveguides on which the lateral flux is null, because of symmetry. Under normally incident waves such configuration is equivalent to that of a single flap in a channel.

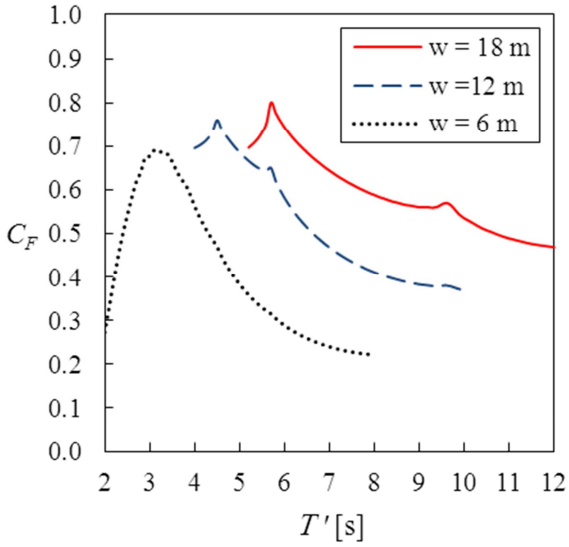

Figure 3 - Capture factor versus period of the incident wave for the channel configuration of Section III – 1. Three different flap widths are considered.

beneficial effect of increasing the maximum capture factor and enlarging the bandwidth of the capture factor curve. This is due to the selective behaviour of the transverse sloshing modes of the system, for which the most powerful modes resonate with the larger flaps [see again 5]. When $w \rightarrow b$, however, such effects are largely inhibited and the system behaves in a "quasi-2D" manner, the capture factor approaching the 2D limit $C_F = 1/2$ [1].

III – 2 An infinite array of flaps in the open ocean

For an infinite array of flaps, the most important design parameter is the gap $a = b - w$ between two adjacent converters (see again figure 2), for given geometry of the flaps and

a/b	0.3	0.4	0.5	0.58	0.7	0.95
$P\ (kW)$	504	564	660	795	574	605
C_F	0.60	0.68	0.79	0.95	0.69	0.73

Table 1 - Power captured and capture factor for an infinite array of converters with different gap widths. The geometry of the system is described in Section III - 2. The optimum configuration is highlighted.

period of the incident wave. Such gap must be designed in order to optimise the interference effects between the flaps and maximise the capture factor. As already shown in [6], the optimum capture factor, obtained for

$$\omega = \sqrt{\frac{C}{I + \mu}} \tag{11}$$

i.e. at body resonance [see 9], can be expressed in terms of the gap width a as

$$C_F^{opt} = \frac{1}{2}\frac{|R_0|}{\cos\delta}\left(\frac{a}{w} + 1\right) \tag{12}$$

where R_0 is the complex reflection coefficient of the system, depending on a as well [see expression 33 of 6], and $\delta = \arg R_0$. Now, for a given flap width w, Renzi & Dias [6] showed that expression (12) reaches the maximum value

$$C_F^{opt} = C_F^{max} = \frac{1}{2}\left(\frac{a}{w} + 1\right), \qquad k(a + w) < 2\pi \tag{13}$$

when all the transverse modes are evanescent, i.e. trapped. Since $a/w > 0$, the maximum capture factor (13) for the array is larger than the 2D limit of ½. Hence the mutual interaction between the flaps, which is responsible for the trapping of energy near the array in the form of short-crested waves, can increase the capture factor of the system [5, 6]. Since the limit (13) increases linearly with a, the optimum spacing a_{opt} can be defined as the upper boundary of the region in which (13) holds, i.e. in practice

$$a_{opt} \simeq \lambda - w, \tag{14}$$

with $\lambda = 2\pi/k$, which can be used as a preliminary design formula [see 6]. Note that (13) is a theoretical upper limit, since the body resonance condition (11) is usually not achieved by large flap-type converters [see 5, 6]. Hence the actual capture factor for the array is usually lower than the theoretical upper limit (13) [6].

Table 1 shows an example of optimisation for an infinite array of flaps, each of width $w = 26\,m$ and placed on a bottom foundation with $c = 1.5\,m$. The water depth is $h = 10.9\,m$, the amplitude of the incident wave is $A_I = 1\,m$ and its period is $T = 7\,s$, corresponding to a wavelength $\lambda = 62\,m$. For these parameters, several layouts, from compact (a/b = 0.30) to sparse (a/b = 0.95), are analysed to determine the optimum array spacing a_{opt}. From table 1, note that the largest power output and capture factor are attained at the optimum configuration $a_{opt}/b = 0.58$, i.e. $a_{opt} = 36\,m$ which indeed corresponds to (14).

IV – Conclusions

A single OWSC in a channel and a periodic array of OWSCs have been analysed in this work by using the semi-analytical model of Renzi and Dias [5, 6]. While both systems have the same analytical solutions for normally incident waves, they have different practical application. For the single flap in the channel, the efficiency of the system, evaluated via the capture factor, has been shown to increase with the flap width, as long as the latter remains small with respect to the channel width. In the array configuration, the width of the flap is set and the gap between adjacent flaps is the design variable. Given the wave period and the flap width, the capture factor can be maximised by varying the distance between the flaps, so that complete trapping of the transverse modes occurs. These results have been obtained under the assumptions that the fluid is inviscid and the flow is irrotational. Viscous effects may reduce the values predicted here, especially near cut-off frequencies.

References

[1] Whittaker T., Folley M. Nearshore oscillating wave surge converters and the development of Oyster. Philosophical Transactions of the Royal Society A. 2012; 370: 345–364.

[2] Henry A., Doherty K., Cameron L., Whittaker T., Doherty R. Advances in the design of the Oyster wave energy converter. In: RINA marine and offshore energy conference London, U.K. 2010.

[3] Henry, A. The hydrodynamics of small seabed mounted bottom hinged wave energy converters in shallow water. PhD thesis, Queen's University Belfast. 2008.

[4] Budal K. Theory of absorption of wave power by a system of interacting bodies. Journal of Ship Research. 1977; 21: 248–253.

[5] Renzi E., Dias F. Resonant behaviour of an oscillating wave energy converter in a channel. Journal of Fluid Mechanics. 2012; 701: 482–510.

[6] Renzi E., Dias F. Relations for an array of flap-type wave energy converters. Applied Ocean Research. 2012; 39: 31–39.

[7] Renzi E., Dias F. Hydrodynamics of the Oscillating Wave Surge Converter in the open ocean. European Journal of Mechanics B/Fluids (submitted). 2012.

[8] Newman J.N. Wave effect on multiple bodies. Hydrodynamics in Ship and Ocean Engineering, RIAM, Kyushu University. 2001.

[9] Mei C.C., Stiassnie, M., Yue D.K.-P. Theory and Applications of Ocean Surface Waves. 2005. World Scientific.